Towards a sustainable approach for sound absorption assessment of building materials: Validation of small-scale reverberation room measurement

Towards a sustainable approach for sound absorption assessment of building materials: validation of small-scale reverberation room measurements [a)]

Authors: Louena Shtrepi[1], Andrea Prato[2]

[1]Politecnico di Torino, Torino, Italy

[2]INRiM - Istituto Nazionale della Ricerca Metrologica, Torino, Italy

e-mail addresses: louena.shtrepi@polito.it, a.prato@inrim.it

Corresponding author: Louena Shtrepi

E-mail address: louena.shtrepi@polito.it

Postal address: Department of Energy (DENERG), Corso Duca degli Abruzzi 24, 10129, Torino, Italy

[a)] Part of this work was presented in Proceedings of the 23rd International Congress on Acoustics, 2019, Aachen, Germany

14

Abstract

The research and development phase of sound absorptive building materials by designers, engineers, acoustic consultants and architects need tools for fast, inexpensive preliminary comparison tests on products or acoustic systems. The existing methods exhibit some drawbacks: the impedance tube (IT) is not suitable for 3D systems, while the full-scale reverberation room (FSRR) requires test samples of large dimensions. To overcome these limitations, this work aims to explore the capabilities of small-scale reverberation rooms (SSRR) of about 3 m^3 located at Politecnico di Torino in evaluating the random-incidence sound absorption coefficient. In order to define the range of application and reliability of the method, the considered factors are the sample area and its orientation on the room floor. Four different materials have been tested by applying IT, FSRR and SSRR. The absorption coefficients data obtained with SSRR are compatible with the FSRR benchmarking in the 400-5000 Hz frequency range for three porous materials, and in the range 1000-5000 Hz for the thin rigid material. Therefore, the SSRR can be considered as a reliable alternative for the sound absorption characterization in these ranges for this kind of materials, leading to several benefits. Among them, samples with reduced size can be evaluated with a cheaper equipment in a short time, increasing the overall economical sustainability of the measurement process; in turn, this can encourage designers and architects to perform acoustical measurements since the very early research and development phase, leading to an overall reduction of design costs and improved product quality.

Keywords: Acoustic measurements; Sound absorption coefficient; Measurement uncertainty; Building materials; Sustainability; Small-scale reverberation room.

1. Introduction

The design process of sound absorptive materials is complemented by a preliminary exploratory phase that requires an immediate feedback on the acoustic performance, i.e. the absorption coefficient. Therefore, adequate tools are needed to accelerate the research and development process, minimize costs, and reduce waste due to dismantled samples after their characterization. The absorption coefficient measurement procedure has been the focus of continuous research that have led to two main standardized methods, i.e. the impedance tube (IT) method defined in ISO 10534 [1] and the full-scale reverberation room (FSRR) method described in ISO 354 [2] and ASTM Standard C423 [3]. However, these methods present several disadvantages: IT does not allow to test 3D systems, while FSRR requires large samples. This paper aims to explore the capabilities of small-scale reverberation rooms (SSRR) in providing accurate estimations of the absorption coefficients with respect to the FSRR benchmarking and in overcoming the above-mentioned drawbacks of existing methods.

The main advantages of a SSRR are the possibility to test samples that are much smaller than 10-12 m^2 and the 6.69 m^2 recommended by the FSRR measurements ($V>200$ m^3) according to ISO 354 [2] and ASTM Standard C423 [3], respectively, and to allow more acousticians, manufacturers and practitioners to build their test facility due to the more feasible construction compared to a FSRR. This, in turn, enables a dramatic reduction of economical and time efforts necessary to perform a FSRR measurement. Moreover, the SSRR can be used to improve the quality of acoustic simulations: novel materials at configurations not available in existing databases can be characterized much more easily [4].

Due to their cost effectiveness, SSRRs have been the focus of research in the automotive sector [5], which usually requires absorption data at medium-high frequencies due to the small size of the involved samples. The research has led to a SAE (Society of Automotive Engineers) standard [6] on the use of small rooms for absorption coefficients measurements. The common size of these rooms

is in the range of 3-10 m^3, and a sample area of 0.4-1.5 m^2 is usually deployed [7]: this leads to nearly 90% reduction of the wasted material for laboratory measurements compared to the FSRR (12 m^2). The sample arrangement in the SSRR requires a shorter set-up time: a single panel is usually sufficient, while in FSRR several panels need to be assembled to reach a 12 m^2 sample. In turn the transportation costs and the related environmental pollution benefit from the reduction in material volume. Moreover, the same samples could be reused to measure other important properties for building materials, e.g. the thermal conductivity [8], since the required sample dimensions are comparable to those used in small-scaled rooms.

Further SSRRs are reported in Rey et al. [9] with a volume of 1.12 m^3 and test sample area of 0.3 m^2, and Pacheco et al. [10] with a volume of 0.96 m^3 and test sample area of 0.3 m^2. These scaled rooms have been useful also for testing more complicated structures, e.g. 3D rigid polyester systems, which is difficult to test in an impedance tube [11]. The continuous research on SSRRs has led to the Alpha Cabin, built by the Swiss company Rieter, with a volume of 6.5 m^3. The design and size of the Alpha Cabin is 1:3 scale of the large reverberation room located in the Swiss Federal Laboratory of Material Testing and Research Institute (EMPA). It is largely used in the automotive industry allowing to measure 1.2 m^2 of flat samples or 3D moulded finished parts providing accurate measurements in the frequency range of 400-5000 Hz [11].

A few studies have also compared small-scale reverberation room measurements with those performed in a full-scale reverberation room [9, 11-13]. A good match of the results has been shown in the range of frequencies above 400 Hz, where the SSRR is expected to fulfil the perfect diffusion conditions, i.e. where the degree of diffusion is close to 1. However, these studies also highlight larger discrepancies at low frequencies due to the reduced size of the room. This is a critical aspect since the resulting smaller sample area with equal height produces a larger edge effect [14, 15]. The impact of these effects is particularly high at low frequencies if highly absorbing materials with high thicknesses are tested.

Therefore, two main concerns appear when dealing with small reverberation rooms. The first is related to the lack of a degree of diffusivity of the sound field required to make the measurement conditions largely independent of the room properties [16]. To mitigate this issue, usually different types of diffusers are introduced [2, 17,18]; nevertheless, the efficiency of the diffusers is shown to be reduced when the frequency decreases [19]. In addition, according to Scrosati et al. [20], the diffusers change the mean free path in the reverberation room, thus ISO 354 formula for the calculation of the equivalent absorption area is no longer valid since it does not take into account the actual mean free path and consequently the changed volume of the room. However, low diffusivity of reverberation rooms is still one of the main concerns of the ISO 354 measurements related to the low reproducibility values among laboratories. This is much evident at low frequencies [21], but appear even above the Schroeder frequency, where the sound field should reach a higher degree of diffusivity [22, 23]. One of the causes is due to the fact that the sound field is diffuse in the empty room, while in the room with a highly absorbing sample the sound field cannot be considered perfectly diffuse [20]. For this reason, the diffuse field conditions differences among laboratories has been questioned lately aiming at new requirements to be defined in terms of diffusivity for qualified laboratories [24]. Several studies have shown that large discrepancies might occur among different full-scale laboratories even though they fulfil the ISO qualification requirements [25]. As for FSRR, the low frequencies range in SSRR is the most critical one, where the early decay is dependent on strong, distinct reflections and need to be treated with specific methods [26, 27].

The second drawback of SSRR measurements is related to the diffraction due to the finite size of the tested material, especially at the low frequencies, which is known as the edge effect [14, 28, 29], and restricts the reliability frequency range at medium-high frequencies. Further investigation is needed to clarify the trade-off between reduced sample size and the appropriate room and sample conditions to obtain reliable results for building materials.

To shed light in this direction, this study examines a broad measurement campaign in a small-scale reverberation room in the laboratories of the Department of Energy (DENERG) of Politecnico di Torino, with the aim to evaluate the reliability of the sound absorption coefficient measurements. Four different materials at three different sizes and orientations on the room floor have been tested. The work assesses the compatibility of the SSRR measurements towards measurements made on the same materials in a full-scale reverberation room (ISO 354) [2] at INRiM (Istituto Nazionale di Ricerca Metrologica). Moreover, the same materials have been additionally characterized with the impedance tube method (ISO 10534-2) [1] in order to present an easier and direct comparison towards another standardized method. Finally, the single sound absorption indices α_w (weighted sound absorption coefficient), NRC (Noise Reduction Coefficient), and SAA (Sound Absorption Average), which are used to assess the quality of the absorption and to select products by designers and architects, are derived from the three measurement methods.

2. Methods

The research has been organized through the following steps:

1) Selection of materials and preparation of samples for the measurements in IT, FSRR and SSRR;
2) Measurement of sound absorption in the IT according to ISO 10534-2 [1] and FSRR according to ISO 354 [2];
3) Measurement of sound absorption in the SSRR and test the range of application of ISO 354 [2] method by varying the area of the sample and its orientation on the room floor;
4) Evaluation of the compatibility of the measured SSRR data with the results from IT and FSRR;
5) Computation of the indices α_w, SAA and NRC for the IT, FSRR and SSRR data and compatibility assessment.

2.1 Tested Materials

Four materials (here labelled A, B, C, D) available at INRiM have been tested (Figure 1). Materials A and B are made of glass wool panels with a density of 80 kg/m^3 and a 6 mm finished layer made of glass spheres and a marble powder with overall thickness of 40 mm and 50 mm, respectively. Material C is a 21 mm thick panel with a layer of 13 mm of plasterboard and 8 mm finished layer made of a marble powder. Material D is composed of two superimposed layers of polyester fibre with a density of 80 kg/m^3 and a thickness of 30 mm each. Also, this material has a cellular glass finish of 7.5 mm over the upper layer, and a mixture of rubber and concrete layer of 7.5 mm at the bottom. Since all these materials are obtained by layers of different characteristics, they can be considered as non-isotropic. The four materials have been chosen based on commercially available materials in order to have four different thicknesses: two similar materials A and B with the same layers characteristics but with slightly different thickness, material C considered as a thin rigid material and material D was chosen in order to test the SSRR also for significant thicknesses.

A	B	C	D
Glass wool panels with a finish of 6 mm of glass spheres and a marble powder	Glass wool panels with a finish of 6 mm of glass spheres and a marble powder	Panel with a layer of plasterboard and one of 8 mm of marble powder	Double layered Polyester fiber panel; cellular glass finish of 7.5mm over the upper layer, and a mixture of rubber and concrete layer of 7.5mm at the bottom
Thickness: 40mm	Thickness: 50 mm	Thickness: 21 mm	Thickness: 75 mm
Mass density per unit area: 7.30 kg/m^2	Mass density per unit area: 7.70 kg/m^2	Mass density per unit area: 14.15 kg/m^2	Mass density per unit area: 7.10 kg/m^2

Fig. 1. Sample A and B: Glass wool panels with a finish of glass spheres and a marble powder (40 mm and 50 mm). Sample C: one layer of plasterboard and one of marble powder (21 mm). Sample D: Double layered polyester fibre panel with a cellular glass finish (75 mm).

2.2 Impedance tube measurements

Measurements have been performed in the impedance tube in accordance with ISO 10534-2 [1] (two-microphone technique) in order to measure the normal-incidence absorption coefficient (α_0) for the four materials. The advantages of this method rely on the possibility to obtain measurements using small samples of less than 0.1 m^2 that are easily obtained and introduced into the impedance tube. These measurements took place in the INRiM laboratory. Two different tubes of 30 mm and 50 mm diameter each (Figure 2), both equipped with two ¼'' microphones (Brüel & Kjær 4136), have been used in order to assure a higher accuracy in the whole frequency range of interest, i.e. 100-5000 Hz. The 30 mm tube (length of 45 cm and microphone spacing of 16 mm) allows to measure with a high accuracy in the frequency range of 400-6300 Hz and the 50 mm tube (length of 52 cm and microphone spacing of 26 mm) in the frequency range of 100-3150 Hz. The ISO 10534-2:2001 standard does not define the exact frequency range for a given tube diameter and microphone separation, but recommends the bounds for the lower and upper frequencies; therefore, the frequency range was chosen to satisfy the standard requirements for the level of nonlinearities, frequency resolution, measurement instabilities and signal-to-noise ratio [30].

Both the two tubes are equipped with a white noise source which generates a flat spectrum in the 100-5000 Hz frequency range. The possible gaps among the sample perimeter and the tubes inner surfaces have been sealed by covering the sample border with vaseline without creating local compression on the samples. In this way, the size of the voids between the tested material and the sample holder was reduced so that the circumferential effect discussed in [31] could be considered negligible. The effect of the irregularities in the samples, and in particular at the edges, was taken

into consideration by repeating the tests with three different samples. Temperature and atmospheric pressure were measured with proper calibrated transducers. For each material type, measurements were performed on three samples (nominally equal), obtained from the same larger sample, in order to evaluate uncertainty contribution due to reproducibility.

The normal-incidence absorption coefficients (α_0) data from the two tubes measurements have been combined in order to fulfil their covered frequency range, thus considering the values from the 50 mm tube in the range 100-315 Hz; the mean values from the two tubes in the range 400-3150 Hz and the values from the 30 mm tube in the range 4000-5000 Hz. These data are shown in Appendices A, B, C and D as IT_n.

These values have been corrected for diffuse incidence based on the approach proposed in Spagnolo and Benedetto [32], which uses a physical model to determine the random-incidence absorption coefficient (α) by integrating a vector of evenly spaced 90 angles between 0° and 90°, i.e. the whole hemi-solid angle, allowing to estimate the sound energy density absorption at each angle of incidence, randomly, as in near-diffuse field, according to Eq. (1). There are several methods that can be used to perform this correction taking into account the finite sample size [33] and a different angular integration limit [34].

$$\alpha = \int_0^{\pi/2} \alpha_\theta \cos\theta \, d\theta \tag{1}$$

where θ is the angle of incidence of the pressure waves on the sample and α_θ is the sound absorption coefficient at angle θ given by Eq. (2);

$$\alpha_\theta = 1 - \left| \frac{Z\cos\theta - \rho_0 c}{Z\cos\theta + \rho_0 c} \right|^2 \tag{2}$$

where Z, assuming locally reacting surface, is the acoustic impedance of the absorbing material given by:

$$Z = \rho_0 c \frac{1 + (1 - \alpha_0)^{1/2}}{1 - (1 - \alpha_0)^{1/2}} \quad (3)$$

where ρ_0 is the density of air, c is the speed of sound, and α_0 is the normal-incidence absorption coefficient evaluated in the impedance tube.

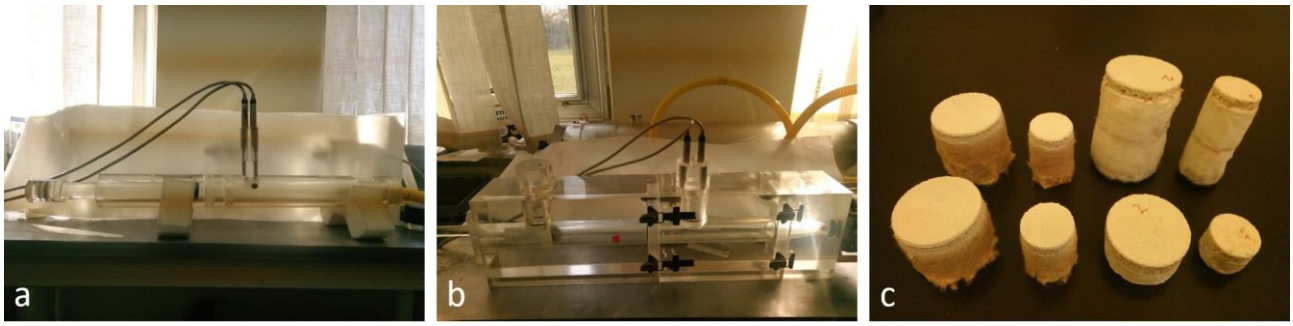

Fig. 2. Measurements set-up in the impedance tube with a diameter of a) 30 mm and b) 50 mm, and c) circular samples of the four materials with a diameter of 30 and 50 mm.

2.3 Full-scale reverberation room measurements

All the materials have been tested in the full-scale reverberation room at INRiM, which is a qualified room for measurements in accordance with ISO 354 [2]. The method allows to estimate the random-incidence absorption coefficient (α_S) in the 100-5000 Hz frequency range. The room has a floor surface of 59.4 m^2 and a height of 4.95 m, which lead to a volume of 294 m^3. Room plan is irregular with non-parallel side walls. The indoor surfaces are characterized by strongly reflective walls and a marble floor characterized by an equivalent sound absorption area lower than 5 m^2 in the 100-5000 Hz frequency range. The mean reverberation time of the empty room between 100 Hz and 5000 Hz is of 10.3 s, thus the Schroeder frequency f_s is 374 Hz. Five diffusers are hung over the ceiling in order to assure diffusivity. The tested samples have an area of 12 m^2 and have been located on the floor of the room within a wooden frame, which is recommended to be used to seal the edges of the tested material. In this experiment the frame has been used for all the samples

except for the case of sample C, which has a negligible thickness. The porous layer for this material is of 8 mm, which was taken into account in the estimation of the overall area of the sample by increasing it of 0.11 m^2.

The set-up and the samples of each material have been arranged in accordance with the recommendations of the ISO 354 standard (Figure 3):

- microphones should be positioned at a minimum distance of 1.5 m from each other, 1 m from the room surfaces and 2 m from the sources;
- the two sources must be at least 3 m apart from each other. A spatial averaging is performed considering all the 12 sources and microphones combination;
- the interval of frequencies of interest is reported as third-octave bands in the range 100-5000 Hz;
- controlled conditions of temperature (> 15 °C) and humidity (between 30-90 %);
- the sample must be rectangular with a ratio between width and length within the range 0.7-1. In this specific case, the test specimens were composed of 25 single small panels with size 60×80 cm^2 combined in order to cover an area of 4×3 m^2;
- the sides of the sample must be distant from the walls of the room by at least 1 m.

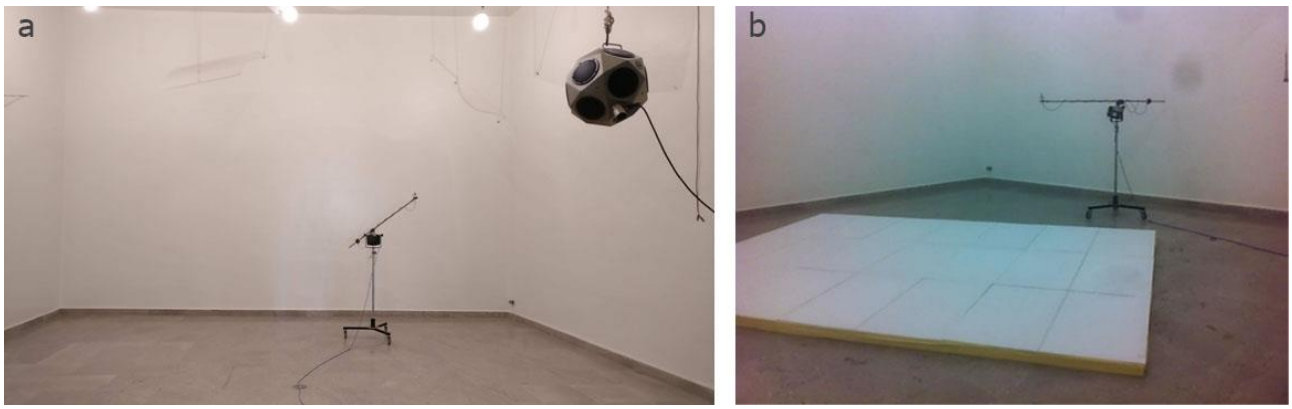

Fig. 3. Measurements in the full-scale reverberation room a) without and b) with the sample.

The procedure consists in using the interrupted noise method [2] on six different microphone positions in two conditions, i.e. with and without the sample on the floor of the room. The measurement chain is composed of a 1/2" microphone (Brüel & Kjær 4943), sequentially located at different positions, and two dodecahedral sources (Brüel & Kjær 4292 and Brüel & Kjær 4296). The applied recording system is the SINUS, Apollo system with software Samurai 2.6; while the sound equalizer is Yamaha (DEQ 5) and the power amplifier is Amcron Crown (MICRO-TECH 1200). In these measurements two sound sources are used for the simultaneous excitation, therefore the number of spatially independent measured decay curves may be reduced to six [2]. For each of the six positions, measurements are repeated four times, and the reverberation time relative to a 20 dB decay, i.e. T_{20}, is evaluated and used to estimate the T_{60}, i.e. the reverberation time occurring for a 60 dB decay. The data are spatially averaged with the ensemble averaging method in order to obtain T_1 and T_2 without and with the sample on the room floor, respectively. The difference between the two measures is used to calculate the variation of the equivalent sound absorption area A_T based on Sabine's theory:

$$A_T = 55.3V\left(\frac{1}{c_2 T_2} - \frac{1}{c_1 T_1}\right) - 4V(m_2 - m_1) \quad (4)$$

where T_1 and T_2 are the reverberation times of the empty reverberation room and after the test specimen has been introduced, respectively; V is the volume of the empty reverberation room; c_1 and c_2 is the propagation speed of sound in air in the room without the sample: $c_1 = 331 + 0{,}6\ t_1$, t_1 is the air temperature; m_1 and m_2 is the power attenuation coefficient of the climatic conditions in the reverberation room without and with the sample (calculated according to ISO 9613-1 [35]);

The random-incidence absorption coefficient is defined as:

$$\alpha_S = \frac{A_T}{S} \quad (5)$$

Where S is the area covered by the test sample.

2.4 Small-scale reverberation room measurements (SSRR)

The small-scale reverberation room (Figure 4, a and Figure 5) is a laboratory at DENERG (Department of Energy, Politecnico di Torino, Italy). It is a 1:5 scale reproduction of the reverberation room described above. The room has been primarily built for random-incidence scattering coefficient measurements according to ISO 17497-1 [36, 37]. It is an oblique angled room with pairs of nonparallel walls. The floor area is about 2.38 m^2 and the height in the range 1-1.2 m, which lead to a maximum volume of 2.86 m^3 and a total area of 12.12 m^2. The structure is raised from the ground on a wooden structure and damping layers have been used along the joints and openings. One of the sides consists of two movable parts that allow to have a large opening to ease the positioning of the sample. The construction material is self-supporting lightweight partitions of MDF (Medium Density Fibreboard) with a thickness of 3.8 cm, which has been further covered by a layer of adhesive film in order to maximize its reflective properties. The equivalent sound absorption area of the empty room (A_1) and ISO [2] and ASTM [3] limits are shown in Figure 4, c. The ISO limit values have been multiplied by the factor $(V/200)^{2/3}$, while the ASTM limit value is given in terms of mean absorption coefficient ($\alpha_m \leq 0.05$ in the 250-2500 Hz interval, and $\alpha_m \leq 0.10$ below 250 Hz and above 2500 Hz) and has been converted into equivalent sound absorption area for comparison purposes. Given that the ISO limit is not specifically indicated for rooms below a volume of 150 m^3, A_1 can be considered acceptable even though slightly above the limit in the range 800-1600 Hz. However, the average absorption coefficient of the indoor surfaces is lower than $\alpha_m=0.05$ in the frequency range of interest (100-5000 Hz). The mean reverberation time of the empty room between 100 Hz and 5000 Hz of 0.95 s, thus the Schroeder frequency f_s is 1152 Hz.

In order to assure a high diffusivity of the sound field [38], 8 diffusers (13.5% of the total room area) have been hung over the ceiling, which is considered as a more economical solution compared

to boundary diffusers leading to an almost equivalent effect on the diffusion of the sound field [18]. A systematic study of the sound field diffusivity evaluation of the room has been performed in [39]. The diffusivity check has been performed in accordance with ISO 354 based on the measurements of the mean absorption coefficient (500-5000 Hz) of a highly sound absorptive panel made of 5 cm thick polyester fibre (Figure 4, d). The final number of diffusers was set to 8, which was a compromise between the rule set by the standard i.e. the mean sound absorption coefficient approaches a constant value (6D to 8D), and limited effect on the volume reduction of the room due to the total coverage of the ceiling, i.e the condition with 10 diffusers (10D).

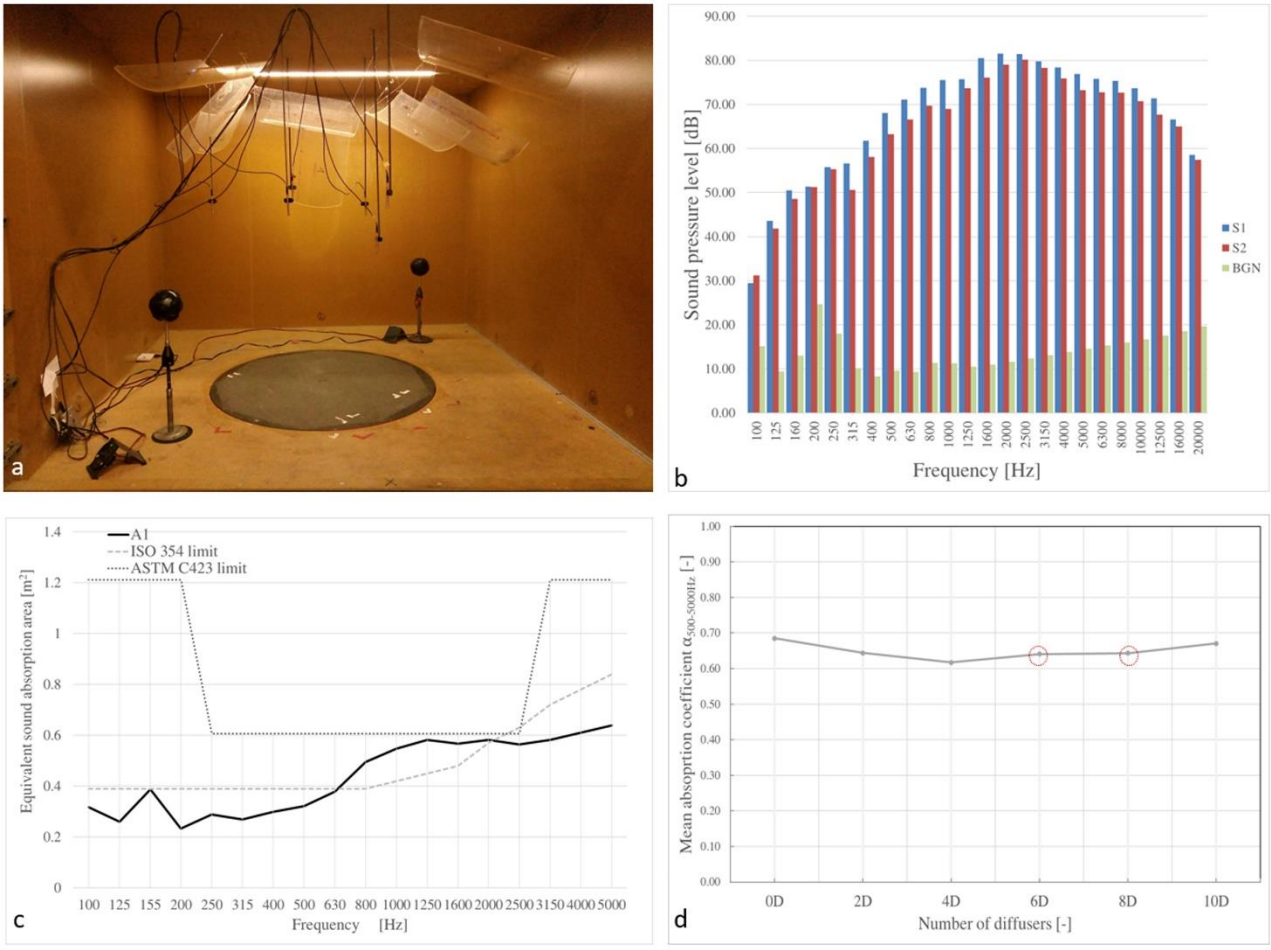

Fig. 4. a) Empty small-scale reverberation room; b) spectral characteristics of the two sound sources (S1 and S2) and background noise; c) comparison of the equivalent sound absorption area of the empty room (A_1), ISO and ASTM limits; d) mean absorption coefficient of a polyester panel of 5 cm measured in the room with no diffusers (0D) and 2-10 diffusers (2D-10D).

The procedure consists in using the integrated impulse response method [2] for simultaneous measurements on six different microphone positions in two conditions, i.e. with and without the sample on the floor of the room as in section 2.3. The measurement chain is composed of six 1/4" BSWA Tech MPA451 microphones and ICP104 (BSWA Technology Co., Ltd., Beijing, China); two ITA High-Frequency Dodecahedron Loudspeakers with their specific ITA power amplifiers (ITA-RWTH, Aachen, Germany) and a sound card Roland Octa-Capture UA-1010 (Roland Corporation, Japan) in order to perform 12 measurements (the minimum number required by ISO 354 [2]). The software used for the measurements, i.e. sound generation, recording and signal processing, is MATLAB combined with the functions of the ITA-Toolbox (an opensource toolbox from RWTH-Aachen, Germany) [40]. The sound source should fulfil the ISO 354 spectral characteristics, that is, the sound pressure levels in the room shall be less than 6 dB in adjacent one-third-octave bands and the level of the excitation signal before the decay shall be sufficiently high so that the lower decibel level of the evaluation range is at least 10 dB above the background noise level, i.e. 35 dB below the initial sound pressure level. The first criterion is fulfilled for the entire frequency range, while the second is fulfilled only above the 250 Hz (Figure 4, b).

For each of the 12 measurements the reverberation time is evaluated. The data are spatially averaged in order to obtain T_1 and T_2 without and with the sample on the room floor, respectively. Equations 4 and 5 are then applied to estimate the random-incidence absorption coefficient.

The set-up and the samples of each material have been arranged in agreement with the recommendations of the ISO 354 standard (Figure 5):

- "microphones should be positioned at a minimum distance of 1.5 m from each other, 1 m from the room surfaces and 2 m from the sources". This leads to 0.3 m; 0.2 m and 0.4 m in 1:5 scale;

- "the two sources must be at least 3 m apart". This leads to 0.6 m in 1:5 scale. A spatial averaging is performed considering all the 12 sources and microphones combination;
- the frequencies of interest are reported as third-octave bands in the range 100-5000 Hz. Given the background noise criterion, this is valid for 250-5000 Hz;
- controlled conditions of temperature (> 15 °C) and humidity (between 30-90 %). A sensor has been installed inside the room;
- "the sides of the sample must be distant from the walls of the room by at least 1 m". This leads to 0.2 m in 1:5 scale;

2.4.1 Sample configuration

One of the aims of this study is to define the sample configuration that could lead to accurate results of the absorption coefficient measurements in the small-scale reverberation room. Given the small size of the SSRR, the sound field is expected to be strongly dependent on the configuration of the measured material. Therefore, it is crucial to define the application range of this type of measurements.

The following variables have been considered, tested and the results have been compared with the IT and FSRR measurements:

- three different sample seizes for each material (60×40 cm^2; 60×60 cm^2; and 60×80 cm^2). It should be noted that the ISO 354 recommends a ratio between width and length in the range 0.7-1;
- three different orientations on the floor (Fig.5) for the 60×40 cm^2 and 60×80 cm^2 sample sizes and two different orientations for sample 60×60 cm^2. Orientation 1 assumed the long edge of the sample parallel to the side wall, orientation 2 assumed the axis of symmetry of the sample aligned over the diagonal of the room floor giving an oblique orientation, and

orientation 3 assumed the long edge of the sample parallel to the rear wall. It should be noted that the ISO 354 standard recommends an oblique orientation (orientation 2).

Three repetitions have been performed for each configuration.

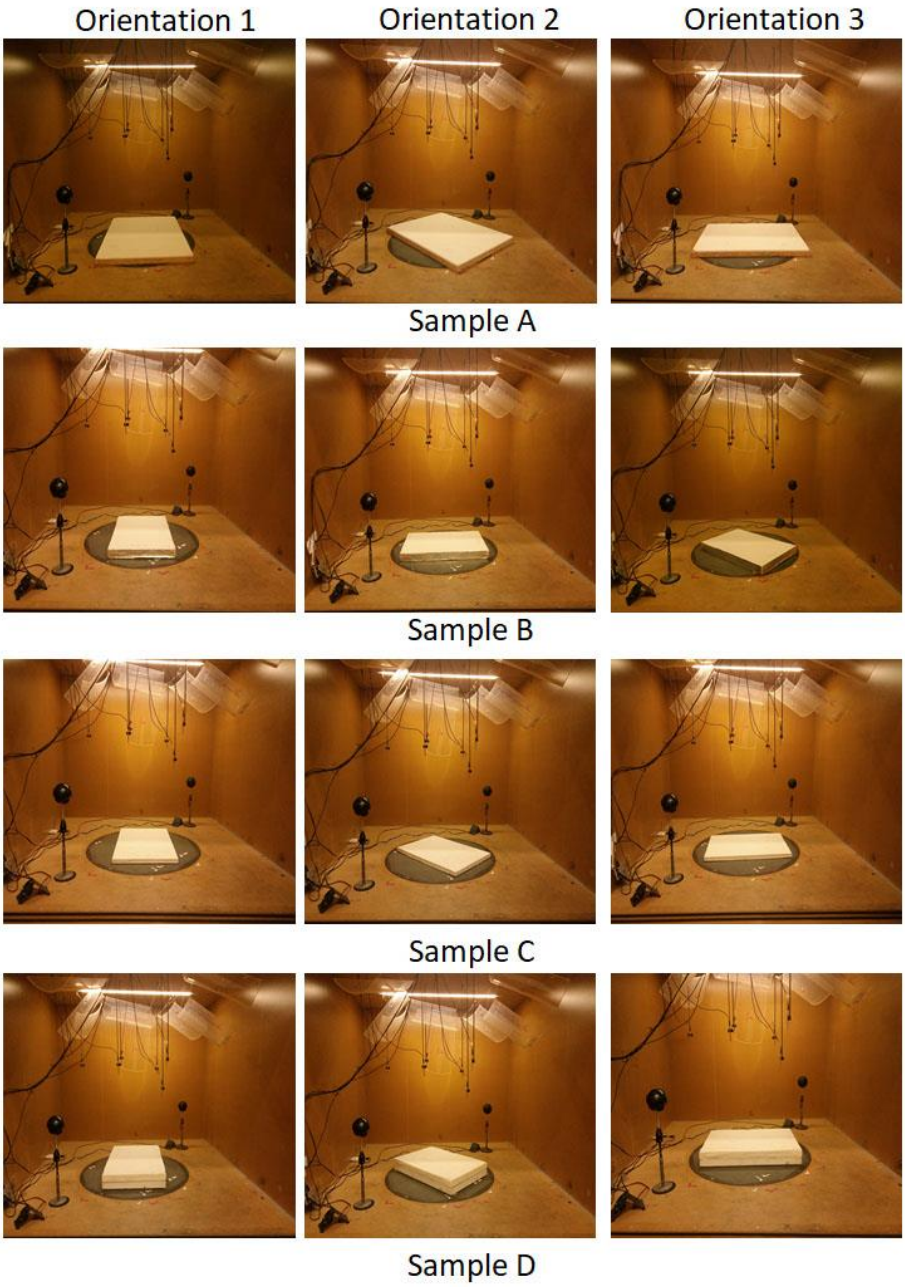

Fig. 5. Measurements in the small-scale reverberation room of one of the samples with three different orientations; Sample A (60×80 cm^2), Sample B (60×40 cm^2), Sample C (60×40 cm^2) and Sample D (60×40 cm^2).

3 Analyses

An analysis based on the estimation of the normalized error (E_n) has been performed in order to assess the compatibility of the absorption coefficient data measured in the SSRR with respect to the FSRR ($E_{n,FSRR}$), considered as reference value for random incidence sound absorption, and IT extended for random-incidence absorption coefficients ($E_{n,IT}$). Moreover, also the normalized error of IT results has been assessed with respect to the FSRR values. E_n is defined as the ratio of the difference between the reference value (α_x) and the reported value (α_y) compared to the root sum square of associated expanded uncertainties (U_x and U_y) at a confidence level of 95% (k=2). According to ISO/IEC 17043:2010 [41], it is evaluated as follows:

$$E_n = \frac{|\alpha_x - \alpha_y|}{\sqrt{U_x^2 + U_{xy}^2}} \quad (6)$$

The data can be considered compatible when $E_n < 1$. This is an indicator of accuracy/inaccuracy as compared to an assigned reference value (FSRR or IT) with respect to the associated uncertainties.

The uncertainty of the impedance tube measurements has been assessed according to GUM-JCGM 100:2008 [42]), taking into account, as type B uncertainty contribution, the difference between the maximum and minimum values coming from the measurement on three nominally equal samples with a uniform rectangular distribution. The specific guidelines given by Wittstock (2018) (see Eq. (2) and Table II – smooth case) [43], which are currently the most reliable reference for the uncertainty evaluation in reverberation rooms based on a database of Interlaboratory Tests, have been applied for the SSRR and FSRR measurement uncertainties. Nevertheless, as shown by the author itself [43], larger uncertainties might occur, especially for highly absorptive materials with ISO 354 method, thus entailing a possible underestimation of the E_n values. Such aspect should be taken into account in the conclusions. The measured frequency dependent absorption coefficients of the four materials and the estimated measurement uncertainties are shown for further details in Appendices A, B, C and D.

The normalized error data have been further analysed with a focus on the effects of the independent factors, i.e. the sample size and orientation. The SPSS Statistics software [44] has been used to perform the ANOVA (ANalysis Of VAriance). The data have been first analysed with a normality test (Kolmogorov-Smirnov test): $E_{n,IT}$ showed a skewness of 0.793 (std.error = 0.105) and kurtosis of 0.004 (std.error = 0.210); $E_{n,FSRR}$ showed a skewness of 0.793 (std.error = 0.105) and kurtosis of 0.004 (std.error = 0.210), thus falling within the acceptable range of ±2 [44].

Moreover, the single indices for sound absorption (α_w, NRC and SAA) are derived from the IT, FSRR and SSRR measurements and compared in terms of compatibility.

Table 1: ANOVA results for $E_{n,IT}$ and $E_{n,FSRR}$ data set.

	$E_{n,IT}$				$E_{n,FSRR}$			
	Size		Orientation		Size		Orientation	
Material	F	p	F	p	F	p	F	p
A	(2, 135) 21.580	0.000	(2, 135) 0.095	0.910	(2, 135) 15.248	0.000	(2, 135) 0.110	0.896
B	(2, 135) 13.910	0.000	(2, 135) 0.093	0.980	(2, 135) 5.496	0.005	(2, 135) 0.090	0.914
C	(2, 135) 0.827	0.440	(2, 135) 0.468	0.628	(2, 135) 0.501	0.607	(2, 135) 0.235	0.791
D	(2, 135) 5.481	0.005	(2, 135) 0.308	0.736	(2, 135) 20.018	0.000	(2, 135) 0.255	0.776

4 Results and discussion

4.1 Effects of the independent factors

The ANOVA performed on the overall E_n set of data showed that the four materials are significantly different from each other at a confidence level of 95% for $E_{n,IT}$ with respect to IT ($F(3, 540) = 14.143$ and $p < 0.001$) and at a confidence level of 90% for $E_{n,FSRR}$ with respect to FSRR ($F(3, 540) = 2.277$ and $p = 0.079$). Therefore, sample size and orientation variables have been analysed for each material separately (Table 1).

The effect of the sample size is statistically significant for all the samples typologies ($p < 0.05$), except for sample C. This result might be due to the limited edge effect for thinner samples, as sample C is 21 mm thick. Appendices A, B, C and D show the absorption coefficient values for each material. For panels with higher thickness (i.e. A, B, D) and when the panel reaches the smallest dimensions 60×40 cm^2, there are evident irregular high peaks at mid and high frequencies for panels A and B, and also at low and mid frequencies for panel D. It can be noticed that the sound absorption increases at 160-400 Hz and above 800 Hz with decreasing samples size (Appendices A, B, and D). This behaviour might be due to a combination of edge effects and to diffusivity effects, caused by the influence of the material on the modal behaviour of the room with and without the sample inside, whereas for low absorbing materials (Appendix C) it can be considered equivalent in terms of spatial distribution and amplification of standing waves. Schiavi and Prato [45] showed these discrepancies by comparing full scale reverberation room, impedance tube, and airflow resistivity methods. The same result has been highlighted also in full-scale rooms by Jain et al. [46], for samples size smaller than 1 m^2, which is due to diffraction occurring at the sample edges. Anyway, in general terms, depending on the sample thickness, the small room gives higher sound absorption values as compared to large reverberation rooms [15]. Samples A, B and D showed this trend above 800 Hz, while sample C above 2000 Hz.

The correct scaling of the sample size with respect to the room volume has been investigated also in Veen et al. [28]. This study shows that a sample of 1.12 m^2 could be considered in order to have reliable results in a small reverberation room with a volume of about 6.4 m^3. The ratio between the room volume and the sample area is comparable to the one obtained with the room volume of 2.86 m^3 and the sample size 60×80 cm^2 (0.48 m^2) used in the present study (i.e. ratio ≈ 6).

The effect of the sample orientation has been analysed for all the materials and all the sample sizes. Table 1 shows that the differences due to sample orientations are not statistically significant for all the materials considered ($p > 0.05$). It is therefore possible to choose an oblique panel orientation (Orientation 2), as suggested in the standard for full-scale measurements. Previous research [16] has shown that different orientations may cause discrepancies at lower frequencies (below 400 Hz) and that the smoothest curve is obtained for the oblique orientation, which is the most asymmetric one. This study also highlighted that the other two orientations cause strong peaks in the absorption coefficient, which were unrealistic for the tested porous materials. The authors argued that this behaviour might be due to the parallel orientation of two edges of the material against two side walls of the reverberation room. However, this effect is not fully observed in the study presented in this paper. Some differences between the three orientations are observed at specific frequencies for the smallest sample size, i.e. 60×40 cm^2 (Appendixes A, B, C, and D). Discrepancies at lower frequencies are reduced when the material has lower thickness, i.e. these differences are more evident in the case of panel D, which has a thickness of 75 mm. This finding is coherent with the results of Cops et al. [16], which showed the same discrepancies between different orientations for samples with thickness higher than 100 mm in full-scale measurements.

4.2 Compatibility of SSRR with IT and FSRR data

Figure 6 shows the maximum normalized error values estimated in each third octave band frequency range for the SSRR data with respect to FSRR and IT data. SSRR data are reliable from

250 Hz upward, due to the background noise criterion previously discussed, however, for the sake of completeness, results are reported from 100 Hz. These plots show the E_n for material A, B, C and D at three sample sizes (60×40 cm^2, 60×60 cm^2, and 60×80 cm^2) and Orientation 2 only, since this factor was not found to be statistically significant. The results show that the normalized error (E_n) is minimized for sample size 60×80 cm^2 for all the materials. $E_{n,FSRR}$ values are lower than 1 in the frequency range 400-5000 Hz, for materials A, B and D. Sample C presents $E_{n,FSRR}$ values lower than 1 at 400 Hz and in the frequency range 1000-5000 Hz. Values slightly higher than 1 result between 500 Hz and 800 Hz. As highlighted in the previous section, this might be due to the limited effects of this low absorbing and thinnest sample on the modal behaviour of the room it-self. This result suggests further future investigation on the room diffusivity. The same conclusions can be obtained for $E_{n,IT}$ for materials A, B and C. For what concern material D, it can be noted that $E_{n,IT} <$ 1 only at 500-1000 Hz. This could be due to the fact that IT method tends to underestimate the sound absorption at mid-high frequencies as shown in Appendix and in Figure 6. $E_{n,IT}$ values are higher than $E_{n,FSRR}$ values, which leads to a higher compatibility of the SSRR with respect to the FSRR. These differences are maximized for the thickest material D, i.e. $E_{n,IT} > 1$ and $E_{n,FSRR} < 1$ at 1250-4000 Hz. The same behaviour can be observed also when evaluating the normalized error of the IT data with respect to the FSRR (Figure 7), i.e. $E_n > 1$ at 1600-3150 Hz.

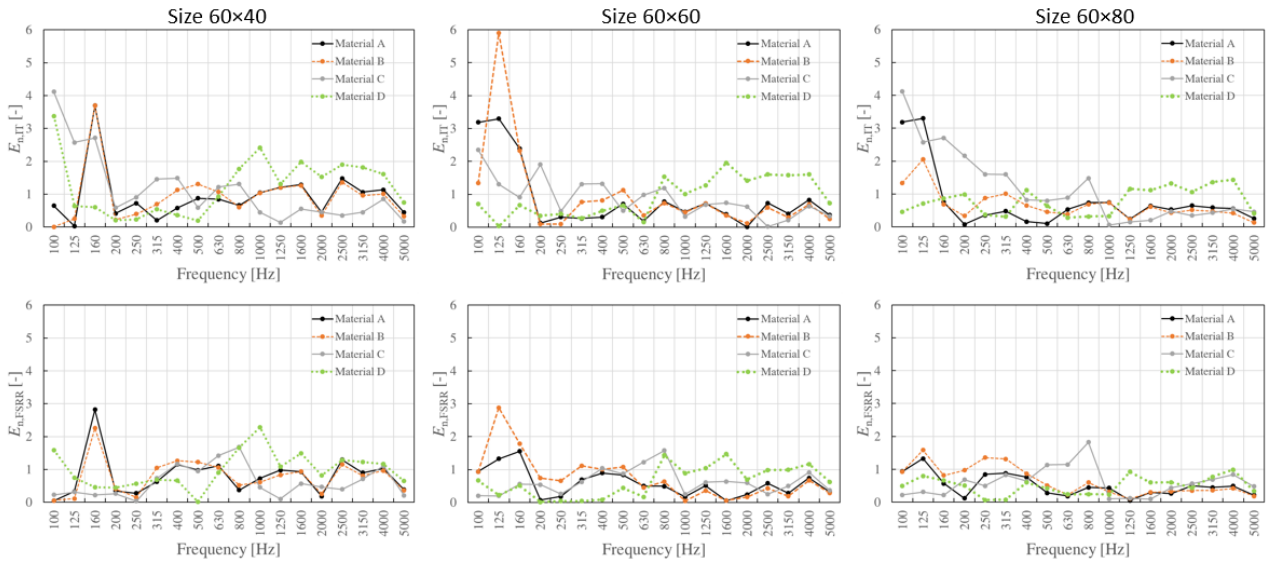

Fig. 6. Normalized error (E_n) for SSRR results (material A, B, C and D) with respect to IT ($E_{n,IT}$) and FSRR ($E_{n,FSRR}$) values for the three sample sizes (60×40 cm^2, 60×60 cm^2, and 60×80 cm^2) and orientation 2. The data can be considered compatible when $E_n < 1$.

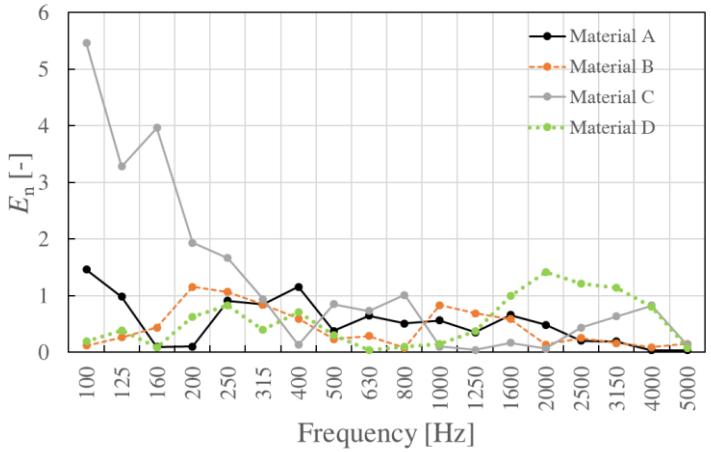

Fig. 7. Normalized error (E_n) for IT results (material A, B, C and D) with respect to the FSRR values. The data can be considered compatible when $E_n < 1$.

The absorption coefficient data of the optimal condition i.e. size 60×80 cm^2 and sample orientation 2, together with the uncertainty values of the results, are shown in Figures 8. The plots show that the SSRR values tend to be higher for frequencies above 800 Hz for samples A, B and D and above 2000 Hz for sample C. One of the causes for this behaviour is that the absorption coefficient approaches to 1 at these frequency ranges and influences the diffusivity of the sound field generated within the small-scale room. This has been observed also in Veen et al. [28], where higher discrepancies around 1000 Hz for samples with thickness above 25 mm were found. Also, Jain et al. [46] showed a good match at mid frequencies from 400-1000 Hz between FSRR and SSRR and an overestimation of sound absorption values above 1000 Hz for the small-scale reverberation room. This is attributed to the use of Sabine's formulas instead of Eyring's as highlighted by Vercammen [21]. Moreover, it should be highlighted that the differences obtained here between the small- and

full-scale room or impedance tube measurements are comparable with those obtained from absorption coefficient measurements in 13 different laboratories Vercammen [21].

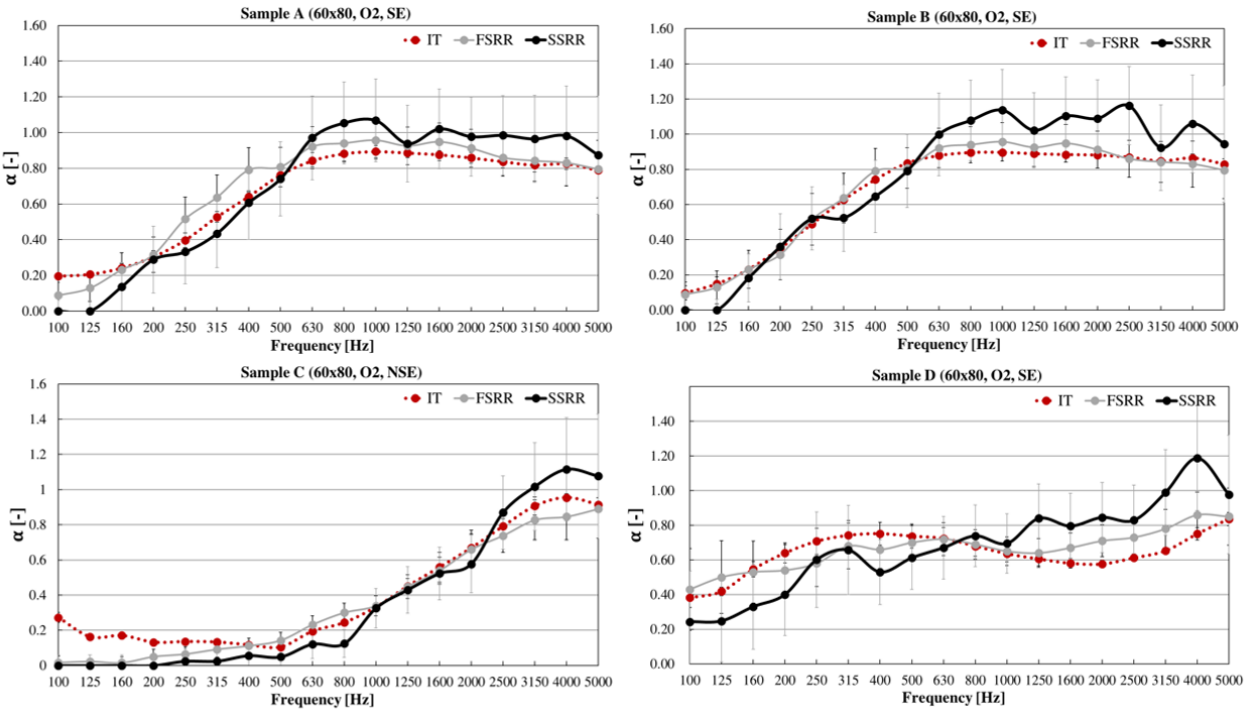

Fig. 8. Absorption coefficient of four materials in the conditions that minimized the normalized error: samples with a size of 60×80 cm^2, orientation 2, with sealed edges (Sample A, B, and D) and with unsealed edges (Sample C). Also, the FSRR data report measurements with sealed edges and no sealed edges, respectively. IT data are given after correction for diffuse incidence.

4.3 Single number acoustic indices α_w, NRC, and SAA

Based on the above results, sound absorption indices α_w, NRC, and SAA are derived from the IT, FSRR and SSRR measurements. These single indices are useful for an immediate and practical comparison of the performance of different materials. The higher the α_w, SAA or the NRC values, the better is the material capability in sound absorption. Their values normally range from 0 to 1, with 1 meaning 100% sound absorption for 1 m^2 of material. These three indices have been compared in former studies in order to estimate the differences and any possible drawback that could lead to flaws in the performance comparison [47].

The weighted sound absorption coefficient α_w is derived from practical sound absorption coefficients, α_p. They are frequency-dependent values of the sound absorption coefficient, based on measurements on one-third octave bands (according to EN ISO 354 [2]) and calculated in octave bands in accordance with EN ISO 11654 [48]. An averaged α_p is calculated for the three one-third octave sound absorption coefficients within the octave. Weighted sound absorption coefficient α_w can be obtained with the reference curve (α_{250}=0.8; α_{500}=1; α_{1000}=1; α_{2000}=1; α_{4000}=0.9). The curve is shifted in steps of 0.05 towards the α_p values until the sum of unfavourable deviations (this occurs when the measured value is lower than the value of the curve) is less or equal to 0.10. Finally, the weighted sound absorption coefficient is the value of the adjusted reference curve at 500 Hz.

The single number rating obtained from ASTM C423 [3] is the Sound Absorption Average (SAA). This is the average of the absorption coefficients for the twelve one-third octave bands from 200 Hz to 2500 Hz. The SAA supersedes the Noise Reduction Coefficient (NRC), which is the arithmetic average of the absorption coefficients determined at the octave bands of 250 Hz, 500 Hz, 1000 Hz and 2000 Hz, rounded to the nearest multiple of 0.05. The SAA value is rounded off the nearest 0.01 increment. The ASTM standard does not introduce any shape indicators as the ISO method described above.

The expanded uncertainty, at a confidence level of 95% (k=2), of the measured data under reproducibility conditions for α_w has been evaluated according to Wittstock (2018) [43] and is equal to 0.07, i.e. twice the reproducibility standard deviation; the same value has been considered also for SAA and NRC, since no information is given on this regard in literature. As can be noticed in table 2, there are a few differences among the single indices within each material data. The differences SSRR and FSRR related to α_w are within a 0.10 for samples A and B, and 0.05 for samples C and D; differences related to NRC and SAA are within 0.05 for all the samples. Table 2 shows also the normalized error which has been evaluated for IT and SSRR measurements with respect to the FSRR data and SSRR with respect to the IT single values. The results can be

considered compatible in most of the cases ($E_n < 1$). However, it can be noticed that the differences between SSRR and FSRR are comparable to those between IT and FSRR.

Table 2: Comparison of results of single acoustic indices (NRC, SAA and α_w) for the four samples (A, B, C, D) and three different test methods (IT, FSRR, and SSRR). Normalized error of the IT and SSRR measurements with respect to the FSRR data and SSRR measurements with respect to IT data. E_n >1 are indicated in bold.

Sample	A			B			C			D		
Test Method	α_w	SAA	NRC	α_w	SAA	NRC	α_w	SAA	NRC	α_w	SAA	NRC
IT	0.70	0.73	0.75	0.75	0.77	0.75	0.20	0.32	0.30	0.65	0.67	0.65
FSRR	0.75	0.79	0.75	0.85	0.84	0.75	0.20	0.31	0.30	0.70	0.66	0.70
SSRR	0.65	0.78	0.80	0.75	0.87	0.85	0.15	0.26	0.25	0.70	0.68	0.70
$E_{n\ (IT\text{-}FSRR)}$	0.51	0.61	0.00	**1.01**	0.71	0.00	0.00	0.10	0.00	0.51	0.10	0.51
$E_{n\ (SSRR\text{-}FSRR)}$	**1.01**	0.10	0.51	**1.01**	0.30	**1.01**	0.51	0.51	0.51	0.00	0.20	0.00
$E_{n\ (SSRR\text{-}IT)}$	0.51	0.51	0.51	0.00	**1.01**	**1.01**	0.51	0.61	0.51	0.51	0.10	0.51

4.4 Comparison among the three methods

Finally, a summary of the advantages and disadvantages of the three methods are listed in Table 3. It can be noticed that the SSRR presents a series of practical advantages that could allow for faster measurements applying less resources, i.e. allows for an explorative phase in the early stages of the design process as well as reduces the amount of material used for the production of the samples leading to more sustainable ways of performing acoustic measurements. Moreover, these practical features and faster feedback could ease the dissemination and increase awareness related to the acoustic performance among designers and architects.

5 Conclusions

This work explored the range of application and reliability of the random-incidence absorption coefficient measured within a small-scale reverberation room. Four different materials have been measured with three different methods in the impedance tube (IT), full-scale (FSRR) and small-

scale (SSRR) reverberation room. It was shown that the SSRR presents several advantages compared to the other methods, which have a practical relevance in the explorative design process of sound absorptive building materials. After the research and development phase, the final material can be sent to an independent acoustical laboratory for qualified ISO 354:2003 measurements.

Table 3: Synthetic comparison among IT, FSRR and SSRR methods.

Method	Sound incidence	Frequency range [Hz]	Sample area (m^2)	Advantages	Disadvantages
IT	Normal	100-5000 (depending on the tube diameter)	< 0.1	• reduced sample size • affordable measurement costs • limited wasted material • measurement time duration (< 30 min)	• limited frequency range • normal sound incidence • 3D absorbing systems
FSRR	Random	100-5000	10-12	• sound incidence • limited edge effect • broad frequency range • 3D absorbing systems	• large sample size • huge measurement costs • high quantity of material to be dismantled • measurement time duration (> 60 min)
SSRR	Random	400-5000 (for porous materials) 1000-5000 (for thin rigid materials)	0.2-1.5	• sound incidence • reduced sample size • affordable measurement costs • limited wasted material • measurement time duration (<30 min) • 3D absorbing systems	• limited lower frequency range • edge effect • limited sample height

The SSRR-based results have been compared against FSRR measurement, used as a reference, and IT measurements. The analyses showed that normalized errors smaller than 1 – i.e. compatible results – can be generally achieved, provided that some recommendations in measurement setup are needed. First, to have reliable data a sample size close to 60×80 cm^2 is recommended; the size

551 should be placed with an oblique orientation on the room floor. Second, the sound absorption
552 coefficients data showed that the edge effect is more evident for thicker panels (>50cm) and smaller
553 samples (60x40cm^2). For samples sizes of 60x80cm^2 the edge effect has been shown to be reduced
554 also for thicker samples. This aspect should be investigated in a more systematic way including
555 panels with thicknesses above those considered here in order to find a threshold of validity due to
556 this parameter. Third, a sound absorption overestimation can take place depending on the sample
557 thickness. Fourth, due to the limited diffusivity of the sound field, the SSRR method can be
558 profitably adopted when the frequencies of interest lie above 400 Hz for porous materials and above
559 1000 Hz for thin low absorptive rigid materials. Nevertheless, as previously stated, since larger
560 uncertainties in SSRRs and in FSRRs might occur especially for higher absorptive materials with
561 ISO 354 method [43], compatibility ranges could be wider. Future research will be aimed at
562 investigating this aspect.
563 Within these use-cases, the discussed results show that that the small reverberation room is a
564 reliable measurement tool in the frequency range 400-5000 Hz (for porous materials) and 1000-
565 5000 Hz (for thin rigid materials), and therefore, can be considered as a valid alternative to the
566 measurements in the full-scale or in the impedance tube. These might require a more systematic
567 study that would consider also other variables (e.g. room volume variations) in order to define the
568 proper range of application.
569 Finally, this work has pointed out the advantages related to the possibility to test small-size
570 samples, thus potentially leading to limited wasted material and transportation costs for the tested
571 samples. Moreover, the sample arrangement in the SSRR set-up requires a shorter time, enabling in
572 turn to dedicate an increased time to test different alternatives. Moreover, this could ease the
573 dissemination and increase awareness related to the acoustic performance among designers and
574 architects while pursuing more sustainable ways to perform acoustic measurements.
575

ACKNOWLEDGEMENTS

The authors are grateful to professors Arianna Astolfi, Marco Masoero and Alessandro Schiavi for the useful discussions and encouragement on this research. They would like to thank the architect Chiara Devecchi, the engineers Paolo Onali and Davide Squarciapino for having provided some of the materials used in these measurements and Francesca Latorella and Andrea Gerbotto for their contribution to the small-scale measurements. The small-scaled reverberation room was built in collaboration with 3F S.r.l..

583

584 **References**

585

586 [1] ISO 10534-2:1998, Acoustics - Determination of sound absorption coefficient and impedance in
587 impedance tubes - Part 2: Transfer-function method. International Organization for
588 Standardization, Geneva, Switzerland.
589 [2] ISO 354:2003, Acoustics - measurement of sound absorption in a reverberation room.
590 International Organization for Standardization, Geneva, Switzerland.
591 [3] ASTM C423-17:2017, Standard Test Method for Sound Absorption and Sound Absorption
592 Coefficients by the Reverberation Room Method, ASTM International, West Conshohocken,
593 PA.
594 [4] A. Alonso, F. Martellotta, Room acoustic modelling of textile materials hung freely in space:
595 from the reverberation chamber to ancient churches, Journal of Building Performance Simulation
596 9 (2016), 469-486. http://dx.doi.org/10.1080/19401493.2015.1087594
597 [5] J. R.Veen, J. Pan, P. Saha, Development of a Small Size Reverberation Room Standardized Test
598 Procedure for Random Incidence Sound Absorption Testing, Proc. SAE conference 2005,
599 Traverse City, USA, 2005.
600 [6] SAE j2883:2015 - Laboratory Measurement of Random Incidence Sound Absorption Tests Using
601 a Small Reverberation Room. SAE International.
602 [7] P. Jackson, Design and Construction of a Small Reverberation Chamber, Proc. SAE conference
603 2005, Traverse City, USA, 2005.
604 [8] G. Baldinelli, F. Bianchi, S. Endelis, A. Jakovics, G. L. Morini, S. Falcioni, S. Fantucci, V. Serra,
605 M. A. Navacerrada, C. Díaz, A. Libbra, A. Muscio, F. Asdrubali, Thermal conductivity
606 measurement of insulating innovative building materials by hot plate and heat flow meter
607 devices: a round Robin test. Int. J. Therm. Sci. 139 (2019), 25-35.
608 https://doi.org/10.1016/j.ijthermalsci.2019.01.037

609 [9] R. Del Rey, J. Alba, L. Bertó, A. Gregoriù, Small-sized reverberation chamber for the
610 measurement of sound absorption, Materiales de Construcción 67 (2017), 139.
611 http://dx.doi.org/10.3989/mc.2017.07316
612 [10] L. Pacheco Bastos, G. Da Silva Vieira de Melo, N. Sure Soeiro, Panels Manufactured from
613 Vegetable Fibers: An Alternative Approach for Controlling Noises in Indoor Environments,
614 Advances in acoustic and vibration 2012, (paper 698737).
615 http://dx.doi.org/10.1155/2012/698737
616 [11] M. Kierzkowski, H. Law, J. Cotterill, Benefits of Reduced-size Reverberation Room Testing.
617 Proc. Acoustics 2017, Perth, Australia, 2017.
618 [12] A. Rasa, Development of a small-scale reverberation room, Proc. Acoustics 2016, Brisbane,
619 Australia, 2016.
620 [13] A. Chappuis, Small size devices for accurate acoustical measurements of materials and parts
621 used in automobiles, Proc. SAE conference 1993; Traverse City, USA, 1993.
622 [14] A. De Bruijn, On the scattering of a plane wave by porous sound-absorbing strip, Proc.
623 Euronoise 2008, Paris, France, 2008.
624 [15] A. Duval, J.-F. Rondwau, L. Dejaeger, F. Sgard, N. Atalla, Diffuse field absorption coefficient
625 simulation of porous materials in small reverberant chambers: finite size and diffusivity issues,
626 Proc. Congres Francais d'Acoustique 2010, Lyon, France, 2010.
627 [16] A. Cops, J. Vanhaecht, K. Leppens, Sound Absorption in a Reverberation Room: Causes of
628 Discrepancies on Measurement Results, Appl. Acoust. 46 (1995), 215-232.
629 https://doi.org/10.1016/0003-682X(95)00029-9
630 [17] M. Nolan, M. Vercammen, C. H. Jeong, Effects of different diffusers types on the diffusivity in
631 reverberation chambers, Proc. Euronoise 2018, Crete, Greece, 2018.

[18] D. T. Bradley, M. Müller-Trapet, J. Adelgren, M. Vorländer, Effect of boundary diffusers in a reverberation chamber: Standardized diffuse field quantifiers. J. Acoust. Soc. Am. 135 (2014), 1898-1906. https://doi.org/10.1121/1.4866291

[19] T.J. Cox, P. D'Antonio, Acoustic Absorbers and Diffusers: Theory, Design and Application, Spon Press, London, United Kingdom, 2004.

[20] C. Scrosati, F. Scamoni, M. Depalma, N. Granzotto, On the diffusion of the sound field in a reverberation room, Proc. 26th International Congress on Sound and Vibration, ICSV, Montréal, Canada, 2019.

[21] M. Vercammen, Improving the accuracy of sound absorption measurements according to ISO 354, Proc. ISRA 2010, Melbourne, Australia 2010.

[22] W. A. Davern, P. Dubout, First report on Australasian comparison measurements of sound absorption coefficients, Proc. CSIRIO 1980, Melbourne, 1980.

[23] N.B. Roozen, E.A. Piana, E. Deckers, C. Scrosati, On the numerical modelling of reverberant rooms, including a comparison with experiments, Proc. ICSV 2019, Montréal, Canada, 2019.

[24] M. Nolan, M. Vercammen, C. H. Jeong, J. Brunskog, The Use of a Reference Absorber for Absorption Measurements in a Reverberation Chamber, Proc. Forum Acusticum 2014, Krakow, Poland, 2014.

[25] C. Scrosati, D. Annesi, L. Barbaresi, R. Baruffa, F. D'Angelo, G. De Napoli, M. Depalma, A. Di Bella, S. Di Filippo, D. D'Orazio, M. Garai, N. Granzotto, V. Lori, F. Martellotta, A. Moschetto, F. Pompoli, A. Prato, P. Nataletti, F. Scamoni, A. Schiavi, F. Serpilli, Design Principles of the Italian Round Robin Test on Reverberation Rooms, Proc. of ICA 2019, Aachen, Germany, 2019.

[26] A. Prato, F. Casassa, A. Schiavi, Reverberation time measurements in non-diffuse acoustic field by the modal reverberation time, Appl. Acoust. 110 (2016), 160-169. https://doi.org/10.1016/j.apacoust.2016.03.041

[27] S. De Cesaris, D. D'Orazio, F. Morandi, M. Garai, Extraction of the envelope from impulse responses using pre-processed energy detection for early decay estimations, J. Acoust. Soc. Am. 138 (2015), 2513-2523. https://doi.org/10.1121/1.4931904

[28] J. R. Veen, P. Saha, Feasibility of a standardized test procedure for random incidence sound absorption tests using a small size reverberation room, Proc. SAE conference 2003, Traverse City, USA, 2003.

[29] T. W. Bartel, Effect of absorber geometry on apparent absorption coefficients as measured in a reverberation chamber, J. Acoust. Soc. Am. 69 (1981), 1065-1074. https://doi.org/10.1121/1.385685

[30] F. Pompoli, P. Bonfiglio, K. V. Horoshenkov, A. Khan, L. Jaouen, F. Bécot, F. Sgard, F. Asdrubali, F. D'Alessandro, J. Hübelt, N. Atalla, C. K. Amédin, W. Lauriks, L. Boeckx, How reproducible is the acoustical characterization of porous media?, J. Acoust. Soc. Am. 141 (2017), 945-955. https://doi.org/10.1121/1.4976087

[31] D. Pilon, R. Panneton, F. Sgard, Behavioural criterion quantifying the effects of circumferential air gaps on porous materials in the standing wave tube, J. Acoust. Soc. Am. 116 (2004), 344-356. https://doi.org/10.1121/1.1756611

[32] R. Spagnolo, G. Benedetto, Reverberation time in enclosures: The surface reflection law and the dependence of the absorption coefficient on the angle of incidence, J. Acoust. Soc. Am. 77 (1985), 1447-1451. https://doi.org/10.1121/1.392039

[33] P. Bonfiglio, F. Pompoli, R. Lionti, A reduced-order integral formulation to account for the finite size effect of isotropic square panels using the transfer matrix method, J. Acoust. Soc. Am. 139 (2016), 1773-1783.

[34] C-H. Jeong, Non-uniform sound intensity distributions when measuring absorption coefficients in reverberation chambers using a phased beam tracing. J. Acoust. Soc. Am. 127 (2010), 3560–3568.

[35] ISO 9613:1993, Acoustics – attenuation of sound during propagation outdoors – Part 1: calculation of the absorption of sound by the atmosphere. International Organization for Standardization, Geneva, Switzerland.

[36] ISO 17497-1:2004, Acoustics – sound-scattering properties of surfaces – Part 1: measurement of the random-incidence scattering coefficient in a reverberation room. International Organization for Standardization, Geneva, Switzerland.

[37] L. Shtrepi, A. Astolfi, G. D'Antonio, G. Vannelli, G. Barbato, S. Mauro, A. Prato, Accuracy of the random-incidence scattering coefficient measurement. Appl. Acoust. 106 (2016), 23-35. https://doi.org/10.1016/j.apacoust.2015.12.021

[38] C. -H. Jeong, Diffuse Sound Field: Challenges and Misconceptions. Proc. INTER-NOISE 2016, Hamburg, Germany.

[39] A. Gerbotto, Caratterizzazione di una camera riverberante in scala - Acoustic characterization of a scaled reverberation room, Master Thesis, Politecnico di Torino, 2016.

[40] ITA-Toolbox for MATLAB® Developed at the Institute of Technical Acoustics at RWTH Aachen University.

[41] ISO/IEC 17043:2010, Conformity assessment - General requirements for proficiency testing. International Organization for Standardization, Geneva, Switzerland.

[42] JCGM 100 2008 Evaluation of Measurement Data — Guide to the Expression of Uncertainty in Measurement (*GUM)*, Joint Committee for Guides in Metrology, Sèvres, France.

[43] V. Wittstock, Determination of Measurement Uncertainties in Building Acoustics by Interlaboratory Tests. Part 2: Sound Absorption Measured in Reverberation Rooms, Acta Acust. United with Acust. 104 (2018), 999 – 1008. https://doi.org/10.3813/AAA.919266

[44] D. George, P. Mallery, SPSS for Windows Step by Step: A Simple Guide and Reference 17.0 Update. 10th Edition, Pearson, Boston, 2010.

[45] A. Schiavi and A. Prato, Valuation of sound absoprtion: an experimental comparative study among reverberation room, impedance tube and airflow resistivity-based models, Proc. ICSV 2019, Montréal, Canada, 2019.

[46] Jain, S., Joshi, M., Bankar, H., Kamble, P., Yadav P., Karanth N. Measurement and Prediction of Sound Absorption of Sound Package Materials in Large and Small Reverberation Chambers, Proc SAE conference 2017, Traverse City, USA, 2017.

[47] J. Białek, E. Nowicka, Comparison of sound absorption ratings calculated according to ISO and ASTM standards, Proc. OSA 2016, Warsaw, Poland, 2016.

[48] ISO 11654:1997, Acoustics - Sound absorbers for use in buildings - Rating of sound absorption. International Organization for Standardization, Geneva, Switzerland.

Appendix A

Sound absorption coefficient (α_s) and related uncertainty (U) for material A measured in SSRR, IT and FSRR. Given the background noise criterion (section 2.4), the SSRR data are valid for 250-5000 Hz. IT_n shows the data for normal-incidence sound absorption coefficients.

SSRR			Frequency [Hz]																	
Size [cm^2]	Orientation		100	125	160	200	250	315	400	500	630	800	1000	1250	1600	2000	2500	3150	4000	5000
60x40	O1	α_s	0.11	0.24	0.00	0.42	0.61	0.53	0.52	0.64	0.68	1.10	1.29	1.10	1.10	1.05	1.13	1.23	1.14	1.04
		U	0.17	0.23	0.06	0.24	0.28	0.22	0.18	0.19	0.18	0.24	0.27	0.24	0.23	0.23	0.24	0.28	0.30	0.35
	O2	α_s	0.10	0.20	0.00	0.40	0.60	0.48	0.53	0.60	0.68	1.03	1.15	1.20	1.20	0.96	1.21	1.10	1.17	0.94
		U	0.15	0.20	0.06	0.24	0.28	0.21	0.19	0.18	0.18	0.23	0.24	0.26	0.25	0.22	0.25	0.26	0.30	0.34
	O3	α_s	0.09	0.17	0.00	0.36	0.58	0.49	0.58	0.56	0.63	1.02	1.05	1.22	1.27	0.90	1.22	1.18	1.15	1.02
		U	0.15	0.18	0.06	0.22	0.27	0.21	0.20	0.17	0.17	0.22	0.23	0.26	0.26	0.21	0.25	0.27	0.30	0.35
60x60	O1	α_s	0.00	0.00	0.01	0.32	0.46	0.51	0.56	0.59	0.70	1.17	0.98	1.04	1.04	0.83	1.00	0.95	0.94	0.85
		U	0.06	0.06	0.06	0.20	0.23	0.21	0.19	0.18	0.19	0.25	0.22	0.23	0.23	0.20	0.22	0.24	0.27	0.33
	O2	α_s	0.00	0.00	0.04	0.33	0.47	0.47	0.58	0.63	0.80	1.06	1.00	1.06	0.96	0.86	1.00	0.92	1.07	0.91
		U	0.06	0.06	0.08	0.21	0.23	0.20	0.20	0.19	0.20	0.23	0.22	0.23	0.21	0.20	0.22	0.24	0.29	0.33
60x80	O1	α_s	0.00	0.00	0.18	0.26	0.38	0.49	0.57	0.72	0.96	1.04	1.08	1.02	1.09	0.92	0.96	0.95	0.97	0.85
		U	0.06	0.06	0.16	0.18	0.20	0.21	0.20	0.20	0.23	0.23	0.23	0.23	0.23	0.21	0.22	0.24	0.28	0.33
	O2	α_s	0.00	0.00	0.14	0.29	0.33	0.43	0.61	0.74	0.97	1.05	1.07	0.94	1.02	0.98	0.98	0.96	0.98	0.87
		U	0.06	0.06	0.14	0.19	0.18	0.19	0.21	0.21	0.23	0.23	0.23	0.21	0.22	0.22	0.22	0.24	0.28	0.33
	O3	α_s	0.00	0.01	0.14	0.24	0.32	0.49	0.56	0.73	0.85	1.07	1.03	0.94	1.05	0.88	0.95	0.92	0.98	0.88
		U	0.06	0.07	0.14	0.16	0.18	0.21	0.19	0.21	0.21	0.23	0.23	0.21	0.23	0.21	0.22	0.24	0.28	0.33
IT		α	0.20	0.21	0.24	0.30	0.40	0.53	0.64	0.76	0.84	0.88	0.89	0.89	0.88	0.86	0.84	0.82	0.83	0.79
		U	0.01	0.02	0.03	0.04	0.04	0.03	0.03	0.04	0.05	0.04	0.03	0.03	0.02	0.03	0.04	0.04	0.03	0.02
IT_n		α_0	0.14	0.15	0.17	0.22	0.30	0.42	0.53	0.66	0.76	0.81	0.83	0.82	0.80	0.78	0.75	0.73	0.74	0.69
		U	0.01	0.02	0.03	0.04	0.04	0.03	0.03	0.04	0.05	0.04	0.03	0.03	0.02	0.03	0.04	0.04	0.03	0.02
FSRR		α_s	0.09	0.13	0.23	0.32	0.52	0.64	0.79	0.81	0.92	0.94	0.96	0.93	0.95	0.91	0.86	0.84	0.83	0.79
		U	0.07	0.08	0.09	0.10	0.12	0.13	0.12	0.11	0.11	0.11	0.11	0.11	0.11	0.11	0.10	0.11	0.13	0.16

Appendix B

Sound absorption coefficient (α_s) and related uncertainty (U) for material B measured in SSRR, IT and FSRR. Given the background noise criterion (section 2.4), the SSRR data are valid for 250-5000 Hz. IT_n shows the data for normal-incidence sound absorption coefficients.

SSRR			Frequency [Hz]																	
Size [cm^2]	Orientation		100	125	160	200	250	315	400	500	630	800	1000	1250	1600	2000	2500	3150	4000	5000
60x40	O1	α_s	0.11	0.24	0.00	0.42	0.61	0.53	0.52	0.64	0.68	1.10	1.29	1.10	1.10	1.05	1.13	1.23	1.14	1.04
		U	0.17	0.23	0.06	0.24	0.28	0.22	0.18	0.19	0.18	0.24	0.27	0.24	0.23	0.23	0.24	0.28	0.30	0.35
	O2	α_s	0.10	0.20	0.00	0.40	0.60	0.48	0.53	0.60	0.68	1.03	1.15	1.20	1.20	0.96	1.21	1.10	1.17	0.94
		U	0.15	0.20	0.06	0.24	0.28	0.21	0.19	0.18	0.18	0.23	0.24	0.26	0.25	0.22	0.25	0.26	0.30	0.34
	O3	α_s	0.09	0.17	0.00	0.36	0.58	0.49	0.58	0.56	0.63	1.02	1.05	1.22	1.27	0.90	1.22	1.18	1.15	1.02
		U	0.15	0.18	0.06	0.22	0.27	0.21	0.20	0.17	0.17	0.22	0.23	0.26	0.26	0.21	0.25	0.27	0.30	0.35
60x60	O1	α_s	0.00	0.00	0.01	0.32	0.46	0.51	0.56	0.59	0.70	1.17	0.98	1.04	1.04	0.83	1.00	0.95	0.94	0.85
		U	0.06	0.06	0.06	0.20	0.23	0.21	0.19	0.18	0.19	0.25	0.22	0.23	0.23	0.20	0.22	0.24	0.27	0.33
	O2	α_s	0.00	-0.09	0.04	0.33	0.47	0.47	0.58	0.63	0.80	1.06	1.00	1.06	0.96	0.86	1.00	0.92	1.07	0.91
		U	0.06	-0.01	0.08	0.21	0.23	0.20	0.20	0.19	0.20	0.23	0.22	0.23	0.21	0.20	0.22	0.24	0.29	0.33
60x80	O1	α_s	0.00	0.00	0.18	0.26	0.38	0.49	0.57	0.72	0.96	1.04	1.08	1.02	1.09	0.92	0.96	0.95	0.97	0.85
		U	0.06	0.06	0.16	0.18	0.20	0.21	0.20	0.20	0.23	0.23	0.23	0.23	0.23	0.21	0.22	0.24	0.28	0.33
	O2	α_s	0.00	0.00	0.14	0.29	0.33	0.43	0.61	0.74	0.97	1.05	1.07	0.94	1.02	0.98	0.98	0.96	0.98	0.87
		U	0.06	0.06	0.14	0.19	0.18	0.19	0.21	0.21	0.23	0.23	0.23	0.21	0.22	0.22	0.22	0.24	0.28	0.33
	O3	α_s	0.00	0.01	0.14	0.24	0.32	0.49	0.56	0.73	0.85	1.07	1.03	0.94	1.05	0.88	0.95	0.92	0.98	0.88
		U	0.06	0.07	0.14	0.16	0.18	0.21	0.19	0.21	0.21	0.23	0.23	0.21	0.23	0.21	0.22	0.24	0.28	0.33
IT		α	0.10	0.15	0.23	0.35	0.49	0.63	0.74	0.84	0.88	0.90	0.90	0.89	0.88	0.88	0.87	0.85	0.86	0.83
		U	0.04	0.04	0.02	0.00	0.01	0.01	0.01	0.01	0.01	0.01	0.01	0.01	0.01	0.01	0.01	0.01	0.02	0.03
IT_n		α_0	0.07	0.10	0.17	0.26	0.38	0.52	0.64	0.75	0.81	0.83	0.83	0.82	0.81	0.81	0.79	0.77	0.79	0.74
		U	0.04	0.04	0.02	0.00	0.01	0.01	0.01	0.01	0.01	0.01	0.01	0.01	0.01	0.01	0.01	0.01	0.02	0.03
FSRR		α_s	0.09	0.18	0.28	0.52	0.65	0.75	0.82	0.86	0.91	0.90	0.99	0.96	0.95	0.90	0.90	0.87	0.85	0.80
		U	0.07	0.09	0.11	0.14	0.15	0.14	0.13	0.12	0.11	0.10	0.11	0.11	0.11	0.10	0.11	0.12	0.13	0.16

Appendix C

Sound absorption coefficient (α_s) and related uncertainty (U) for material C measured in SSRR, IT and FSRR. Given the background noise criterion (section 2.4), the SSRR data are valid for 250-5000 Hz. IT_n shows the data for normal-incidence sound absorption coefficients.

SSRR			Frequency [Hz]																	
Size [cm^2]	Orientation		100	125	160	200	250	315	400	500	630	800	1000	1250	1600	2000	2500	3150	4000	5000
60x40	O1	α_s	0.00	0.00	0.00	0.01	0.03	0.02	0.02	0.07	0.10	0.12	0.32	0.38	1.12	1.12	1.12	1.07	1.21	0.98
		U	0.06	0.06	0.06	0.07	0.07	0.07	0.07	0.07	0.08	0.08	0.11	0.12	1.07	1.07	1.07	0.26	0.31	0.34
	O2	α_s	0.00	0.00	0.00	0.08	0.06	0.03	0.02	0.06	0.10	0.14	0.28	0.43	1.21	1.21	1.21	1.02	1.22	0.97
		U	0.06	0.06	0.06	0.09	0.08	0.07	0.06	0.07	0.08	0.08	0.11	0.13	1.18	1.18	1.18	0.25	0.31	0.34
	O3	α_s	0.00	0.00	0.00	0.09	0.07	0.03	0.04	0.08	0.11	0.09	0.30	0.51	1.32	1.32	1.32	1.03	1.15	0.97
		U	0.06	0.06	0.06	0.10	0.09	0.07	0.07	0.08	0.08	0.07	0.11	0.14	1.28	1.28	1.28	0.25	0.30	0.34
60x60	O1	α_s	0.02	0.05	0.05	0.03	0.10	0.04	0.03	0.08	0.11	0.14	0.34	0.46	0.50	0.54	0.82	0.93	1.02	1.02
		U	0.08	0.10	0.09	0.07	0.10	0.07	0.07	0.08	0.08	0.08	0.11	0.14	0.15	0.16	0.20	0.24	0.28	0.35
	O2	α_s	0.04	0.04	0.08	0.01	0.09	0.04	0.03	0.07	0.12	0.14	0.37	0.36	0.44	0.55	0.79	0.96	1.14	1.03
		U	0.10	0.09	0.10	0.06	0.09	0.07	0.07	0.07	0.08	0.08	0.12	0.12	0.14	0.16	0.20	0.24	0.30	0.35
60x80	O1	α_s	0.00	0.00	0.05	0.00	0.02	0.02	0.03	0.06	0.12	0.15	0.30	0.40	0.50	0.57	0.90	1.01	1.12	1.00
		U	0.06	0.06	0.09	0.06	0.07	0.06	0.07	0.07	0.08	0.08	0.11	0.13	0.15	0.16	0.21	0.25	0.29	0.34
	O2	α_s	0.00	0.00	0.00	0.00	0.02	0.03	0.06	0.05	0.12	0.12	0.33	0.43	0.52	0.58	0.87	1.02	1.12	1.08
		U	0.06	0.06	0.06	0.06	0.07	0.07	0.07	0.07	0.08	0.08	0.11	0.13	0.15	0.16	0.21	0.25	0.29	0.35
	O3	α_s	0.00	0.00	0.04	0.00	0.04	0.03	0.05	0.05	0.13	0.15	0.32	0.43	0.44	0.59	0.85	0.90	1.00	1.00
		U	0.06	0.06	0.08	0.06	0.08	0.07	0.07	0.07	0.08	0.08	0.11	0.13	0.14	0.17	0.21	0.24	0.28	0.34
IT		α	0.27	0.16	0.17	0.13	0.14	0.13	0.12	0.10	0.19	0.24	0.33	0.45	0.56	0.67	0.79	0.91	0.95	0.91
		U	0.03	0.02	0.02	0.01	0.01	0.00	0.00	0.00	0.00	0.01	0.02	0.04	0.08	0.10	0.07	0.05	0.01	0.04
IT_n		α_0	0.20	0.11	0.12	0.09	0.09	0.09	0.08	0.07	0.14	0.18	0.25	0.35	0.45	0.56	0.70	0.85	0.92	0.86
		U	0.03	0.02	0.02	0.01	0.01	0.00	0.00	0.00	0.00	0.01	0.02	0.04	0.08	0.10	0.07	0.05	0.01	0.04
FSRR		α_s	0.02	0.02	0.02	0.05	0.06	0.09	0.11	0.14	0.23	0.30	0.34	0.45	0.54	0.66	0.74	0.83	0.85	0.89
		U	0.04	0.04	0.03	0.04	0.04	0.04	0.04	0.04	0.05	0.05	0.06	0.07	0.08	0.09	0.10	0.11	0.13	0.17

Appendix D

Sound absorption coefficient (α_s) and related uncertainty (U) for material D measured in SSRR, IT and FSRR. Given the background noise criterion (section 2.4), the SSRR data are valid for 250-5000 Hz. IT_n shows the data for normal-incidence sound absorption coefficients.

SSRR			Frequency [Hz]																	
Size [cm^2]	Orientation		100	125	160	200	250	315	400	500	630	800	1000	1250	1600	2000	2500	3150	4000	5000
60x40	O1	α_s	0.07	0.28	0.39	0.65	0.78	0.98	1.07	0.74	1.00	1.21	1.36	0.90	0.85	0.95	1.00	1.21	1.20	1.01
		U	0.12	0.26	0.28	0.35	0.34	0.35	0.32	0.21	0.24	0.25	0.28	0.21	0.20	0.22	0.22	0.27	0.30	0.35
	O2	α_s	0.03	0.26	0.38	0.72	0.79	0.93	0.85	0.70	0.94	1.11	1.29	0.88	1.03	0.90	1.05	1.13	1.25	1.10
		U	0.09	0.25	0.27	0.38	0.34	0.34	0.26	0.20	0.23	0.24	0.27	0.20	0.22	0.21	0.23	0.26	0.31	0.35
	O3	α_s	0.00	0.26	0.40	0.70	0.88	0.92	0.90	0.72	0.94	1.19	1.13	0.99	1.02	0.87	0.99	1.04	1.28	0.96
		U	0.06	0.25	0.29	0.37	0.38	0.34	0.28	0.20	0.23	0.25	0.24	0.22	0.22	0.21	0.22	0.25	0.31	0.34
60x60	O1	α_s	0.09	0.37	0.35	0.53	0.68	0.67	0.58	0.67	0.75	0.93	0.91	0.84	0.78	0.98	0.96	0.98	1.26	1.07
		U	0.14	0.33	0.26	0.29	0.30	0.26	0.20	0.19	0.20	0.21	0.21	0.20	0.19	0.22	0.22	0.25	0.31	0.35
	O2	α_s	0.20	0.41	0.37	0.54	0.59	0.67	0.64	0.61	0.76	1.04	0.84	0.87	1.02	0.87	0.97	1.05	1.25	1.09
		U	0.25	0.35	0.27	0.30	0.27	0.26	0.21	0.18	0.20	0.23	0.19	0.20	0.22	0.21	0.22	0.25	0.31	0.35
60x80	O1	α_s	0.15	0.24	0.34	0.33	0.47	0.66	0.53	0.69	0.70	0.69	0.73	0.71	0.72	0.76	0.80	1.05	1.12	0.99
		U	0.21	0.23	0.25	0.21	0.23	0.26	0.19	0.20	0.19	0.17	0.18	0.18	0.18	0.19	0.20	0.25	0.29	0.34
	O2	α_s	0.24	0.25	0.33	0.40	0.60	0.66	0.53	0.61	0.67	0.74	0.69	0.84	0.80	0.85	0.83	0.99	1.19	0.98
		U	0.29	0.24	0.24	0.24	0.28	0.26	0.19	0.18	0.18	0.18	0.17	0.20	0.19	0.20	0.20	0.25	0.30	0.34
	O3	α_s	0.14	0.26	0.38	0.43	0.54	0.65	0.66	0.78	0.68	0.70	0.73	0.59	0.76	0.85	0.86	0.98	1.11	0.92
		U	0.19	0.25	0.27	0.25	0.25	0.26	0.22	0.22	0.18	0.17	0.18	0.16	0.18	0.20	0.21	0.25	0.29	0.34
IT		α	0.38	0.42	0.55	0.64	0.71	0.74	0.75	0.74	0.72	0.68	0.64	0.61	0.58	0.58	0.61	0.65	0.75	0.84
		U	0.06	0.02	0.04	0.06	0.08	0.08	0.07	0.07	0.06	0.06	0.05	0.04	0.03	0.02	0.02	0.01	0.04	0.04
IT_n		α_0	0.29	0.32	0.44	0.53	0.60	0.64	0.65	0.63	0.62	0.57	0.53	0.50	0.47	0.47	0.50	0.54	0.65	0.75
		U	0.06	0.02	0.04	0.06	0.08	0.08	0.07	0.07	0.06	0.06	0.05	0.04	0.03	0.02	0.02	0.01	0.04	0.04
FSRR		α_s	0.43	0.50	0.53	0.54	0.58	0.68	0.66	0.70	0.72	0.69	0.65	0.64	0.67	0.71	0.73	0.78	0.86	0.85
		U	0.24	0.21	0.18	0.15	0.13	0.13	0.11	0.10	0.09	0.09	0.08	0.08	0.09	0.09	0.10	0.11	0.13	0.16